Supplementary Figures

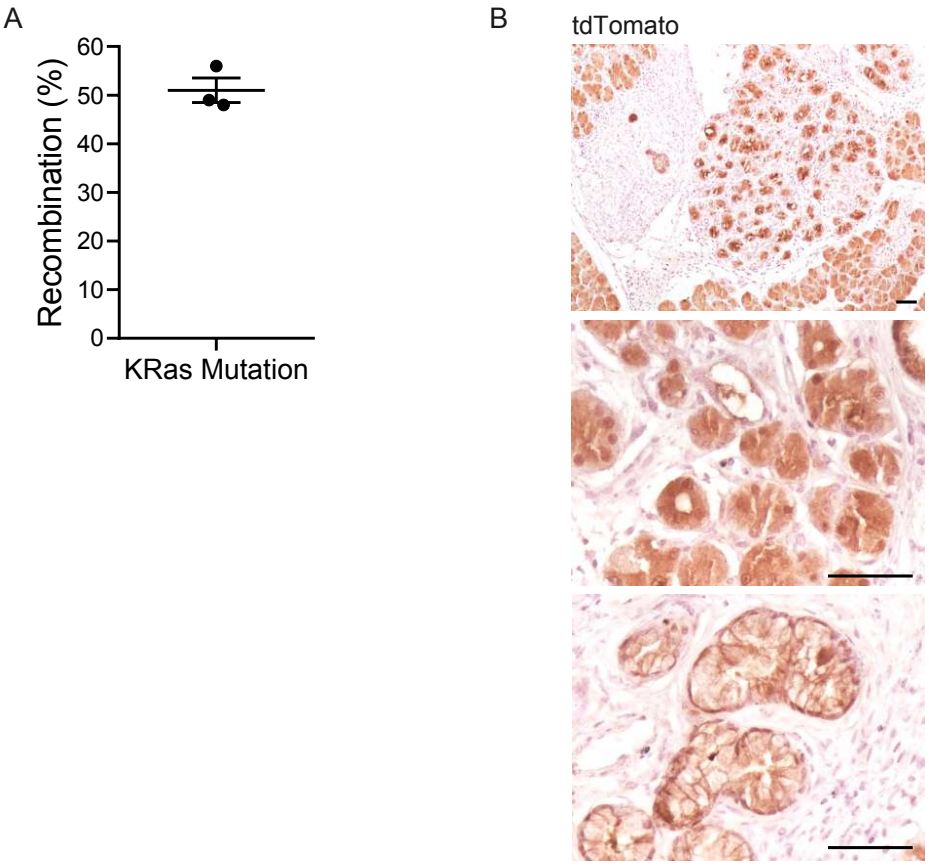

Figure S1. Recombination rates of *LSL-Kras*$^{+/G12D}$ allele. A. Percentage of *LSL-Kras*$^{+/G12D}$ alleles showing recombination, in tdTomato^{+} cells isolated by FACS from pancreata of 3 *Ptf1a-CreER*$^{+/-}$; *LSL-Kras*$^{+/G12D}$; *LSL-tdTomato*$^{+/-}$ mice (dots) 5 days following tamoxifen treatment, as assessed by semi-quantitative PCR conducted on genomic DNA, comparing the ratio of recombined to non-recombined flox alleles. **B.** Representative images (low magnification – top, high magnification – middle and bottom) of PanIN tissues stained with an antibody against tdTomato, showing tdTomato expression in lesion cells and in surrounding acinar cells. Size markers = 50μm.

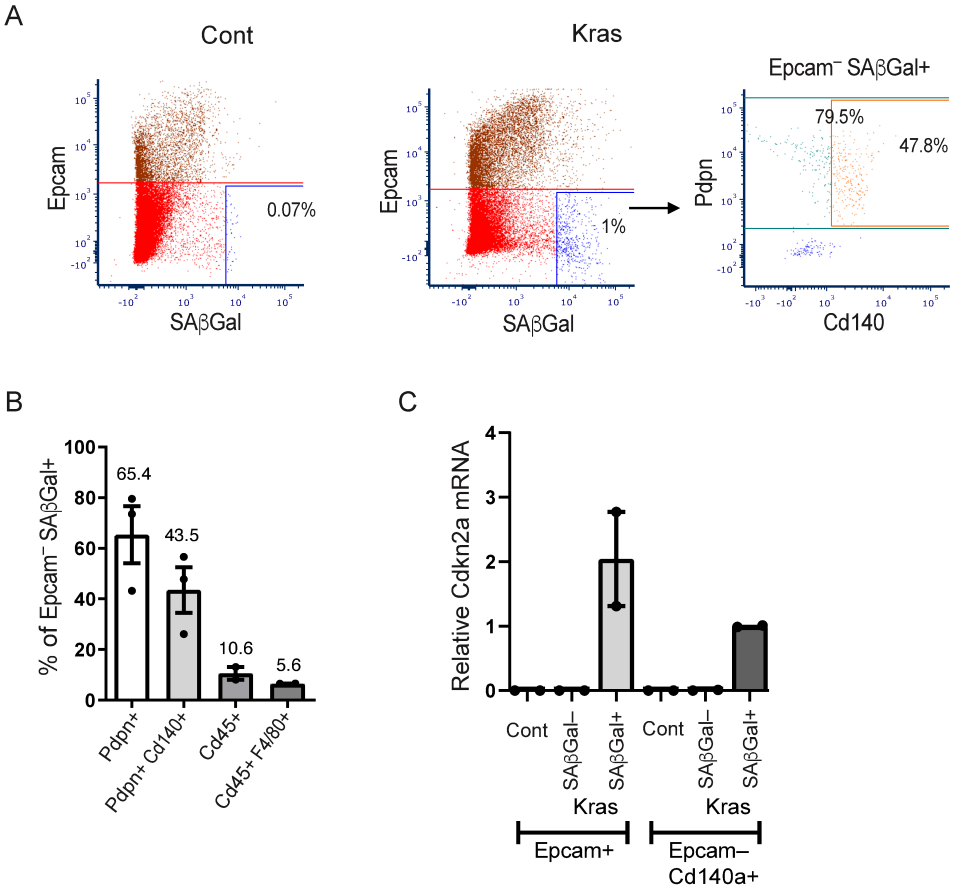

Figure S2. PanIN stroma contains senescent fibroblasts. A. Representative FACS analysis of cells from *Ptf1a-CreER*$^{+/-}$; *LSL-Kras*$^{+/G12D}$ mice 3 months after Kras activation (Kras, right panels) and control *Ptf1a-CreER*$^{+/-}$ mice (left panel, Cont). The tdTomato transgene was replaced by staining for the epithelial marker Epcam. Co-staining of Epcam and SA-βGal, conducted using the fluorescent substrate C_{12}FDG, allowed the characterization and isolation of Epcam^{-} SA-βGal^{high} cells, whose numbers were substantially increased in the Kras-expressing mice versus control mice (gate labeled blue). Staining with the cancer-associated fibroblast markers Pdpn and Cd140a (Pdgfra)[43] (right panel) revealed that the majority of Epcam^{-} SA-βGal^{high} cells are fibroblasts. Percentages on right panel dot plot are of total Pdpn^{+}, or of Cd140a^{+}, out of Epcam^{-} SAβGal^{high} cells. **B.** Percentages of indicated subpopulations out of Epcam^{-} SA-βGal^{high} cells. The Cd140a^{+} fibroblast subpopulation is included in the Pdpn^{+} population; the F4/80^{+} macrophage subpopulation is included in the Cd45^{+} immune population. Values represent mean across individual mice (dots) ± S.E.M. **C.** Expression levels of the *Cdkn2a* senescence marker measured by qRT-PCR in SA-βGal positive and negative subpopulations of Epcam^{+} epithelial compartment and Cd140^{+} fibroblasts, isolated from Kras activated mice, or in corresponding SA-βGal-negative cells isolated from control mice (Cont). Values indicate average of cells sorted from two mice (dots).

43. Elyada E, Bolisetty M, Laise P, et al. Cross-Species Single-Cell Analysis of Pancreatic Ductal Adenocarcinoma Reveals Antigen-Presenting Cancer-Associated Fibroblasts. *Cancer Discov* 2019;9:1102-23.

A

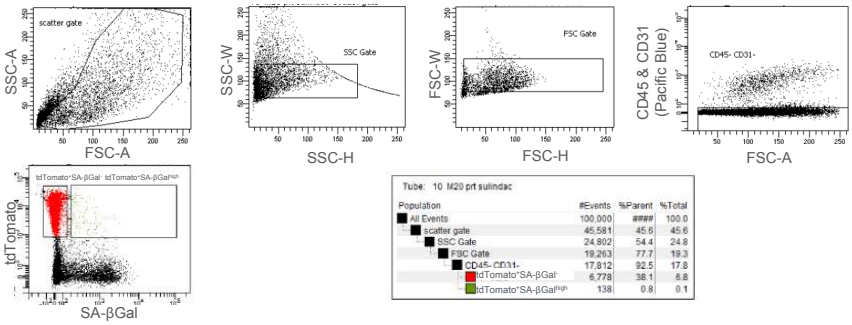
scatter gate
SSC-A
FSC-A
SSC Gate
SSC-W
SSC-H
FSC Gate
FSC-W
FSC-H
CD45- CD31-
CD45 & CD31 (Pacific Blue)
FSC-A
tdTomato
SA-βGal
Tube: 10 M20 prt sulindac
Population #Events %Parent %Total
All Events 100,000 #### 100.0
scatter gate 45,581 45.6 45.6
SSC Gate 24,802 54.4 24.8
FSC Gate 19,263 77.7 19.3
CD45- CD31- 17,812 92.5 17.8
tdTomato+SA-βGal- 6,778 38.1 6.8
tdTomato+SA-βGal++ 138 0.8 0.1

B

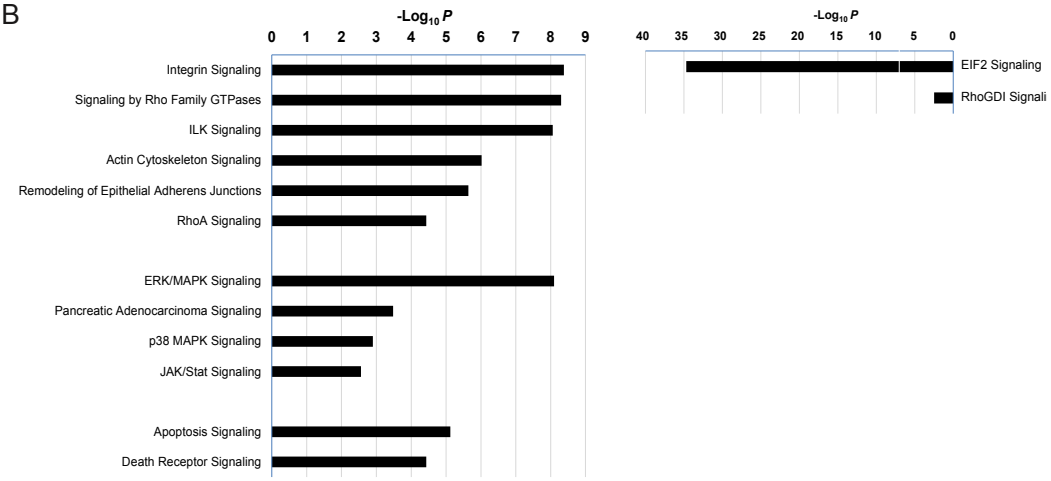
-Log10 P
0 1 2 3 4 5 6 7 8 9
Integrin Signaling
Signaling by Rho Family GTPases
ILK Signaling
Actin Cytoskeleton Signaling
Remodeling of Epithelial Adherens Junctions
RhoA Signaling
ERK/MAPK Signaling
Pancreatic Adenocarcinoma Signaling
p38 MAPK Signaling
JAK/Stat Signaling
Apoptosis Signaling
Death Receptor Signaling
-Log10 P
40 35 30 25 20 15 10 5 0
EIF2 Signaling
RhoGDI Signali

C

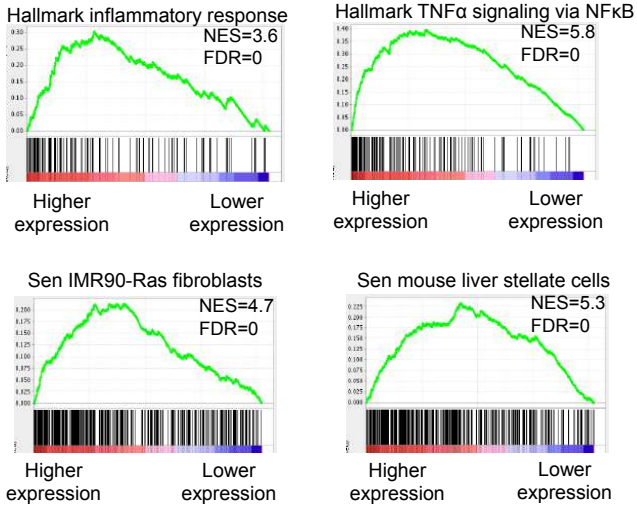
Hallmark inflammatory response
NES=3.6
FDR=0
Higher expression
Lower expression
Hallmark TNFα signaling via NFκB
NES=5.8
FDR=0
Higher expression
Lower expression
Sen IMR90-Ras fibroblasts
NES=4.7
FDR=0
Higher expression
Lower expression
Sen mouse liver stellate cells
NES=5.3
FDR=0
Higher expression
Lower expression

Figure S3. Isolation and profiling of the tdTomato$^+$ SA-βGal^{high} population. A. Sorting procedure for the isolation of senescent and non-senescent PanIN cells, shown on a representative FACS of cells from triple-transgenic *Ptf1a-CreER*$^{+/-}$; *LSL-Kras*$^{+/G12D}$; *LSL-tdTomato*$^{+/-}$ mice 3 months after Kras activation. Following FSC and SSC gating to eliminate cell doublets, cells were gated to exclude CD45$^+$ (hematopoietic) and CD31$^+$ (endothelial) fractions; tdTomato$^+$ SA-βGal$^-$ cells (red, top left), and tdTomato$^+$ SA-βGal^{high} (green, top right) were gated for isolation as indicated. **B.** Additional gene sets upregulated (left) and downregulated (right) in SA-βGal$^+$ versus SA-βGal$^-$ PanIN cells isolated from Kras-activated mice 3 months after tamoxifen treatment. Values indicate $-\log_{10}$ of Adj *P* value as determined by Ingenuity Pathway Analysis. **C.** Gene set enrichment analysis (GSEA) of expression profiles of SA-βGal$^+$ versus SA-βGal$^-$ PanIN cells indicating enrichment for inflammatory (top) and senescent cell (bottom) gene sets.

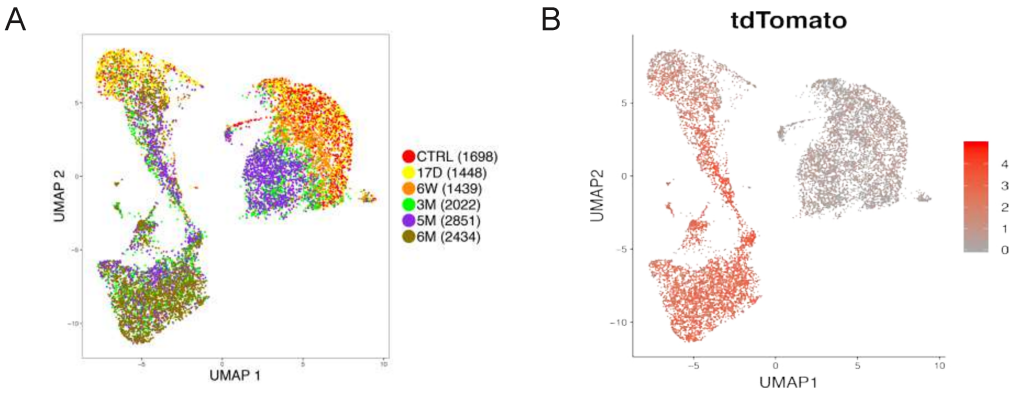

Figure S4. scRNA-Seq of Kras-driven PanINs. A. Uniform manifold approximation and projection (Umap) cell clustering of the scRNA-seq expression profile of epithelial cells from *Ptf1a-CreER*$^{+/-}$; *LSL-Kras*$^{+/G12D}$; *LSL-tdTomato* mice, as shown in Fig. 2I,J. Colors indicate different time points after Kras activation in which cells were collected, as indicated. Cells from *Ptf1a-CreER*$^{+/-}$; *LSL-tdTomato* control mice (CTRL) are labeled red. Numbers of sequenced cells at each time point are indicated in parentheses. **B.** Expression of tdTomato across cells (red – high, grey - low), observed in normal acinar cells as well as PanIN cells.

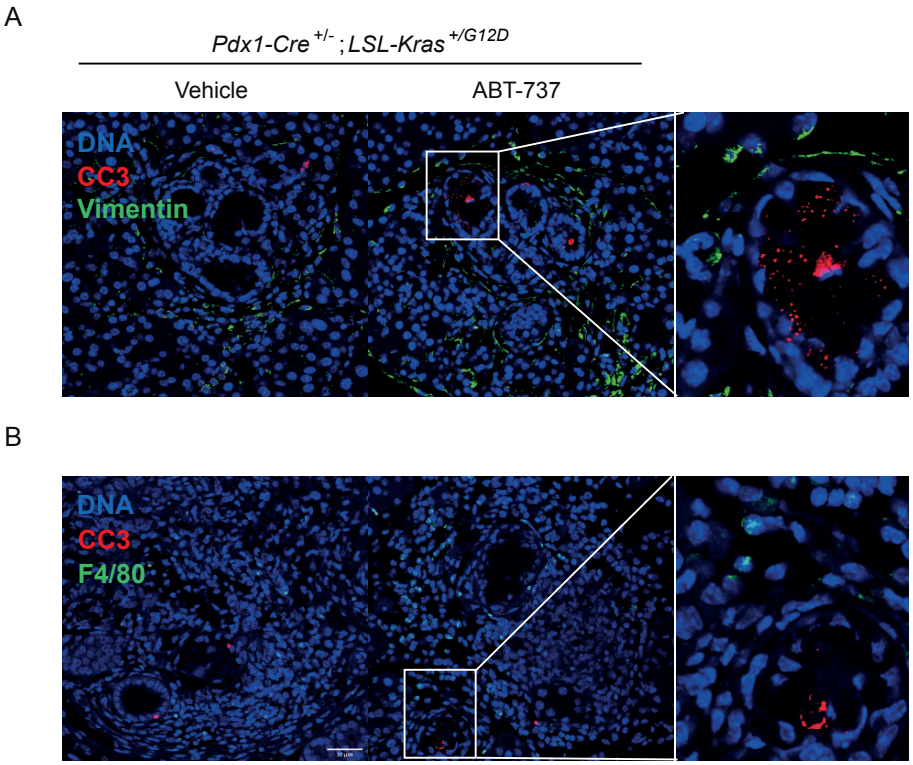

Figure S5. Bcl2-family protein inhibition by ABT-737 does not induce apoptosis in stromal cells. *Pdx1-Cre*$^{+/-}$*;LSL-Kras*$^{+/G12D}$ mice were treated by caerulein at 2.5 months of age, followed by treatment with ABT-737 two weeks subsequently, and analyzed two days later. **A.** Co-staining of pancreas sections from vehicle and ABT-737 treated mice for CC3 (red), and the fibroblast marker vimentin (green), showing no overlap in expression, with CC3 stain detected only within PanIN epithelial ductal structures. **B.** Co-staining of pancreas sections from vehicle and ABT-737 treated mice for CC3 (red), the macrophage marker F4/80 (green) showing no overlap in expression.

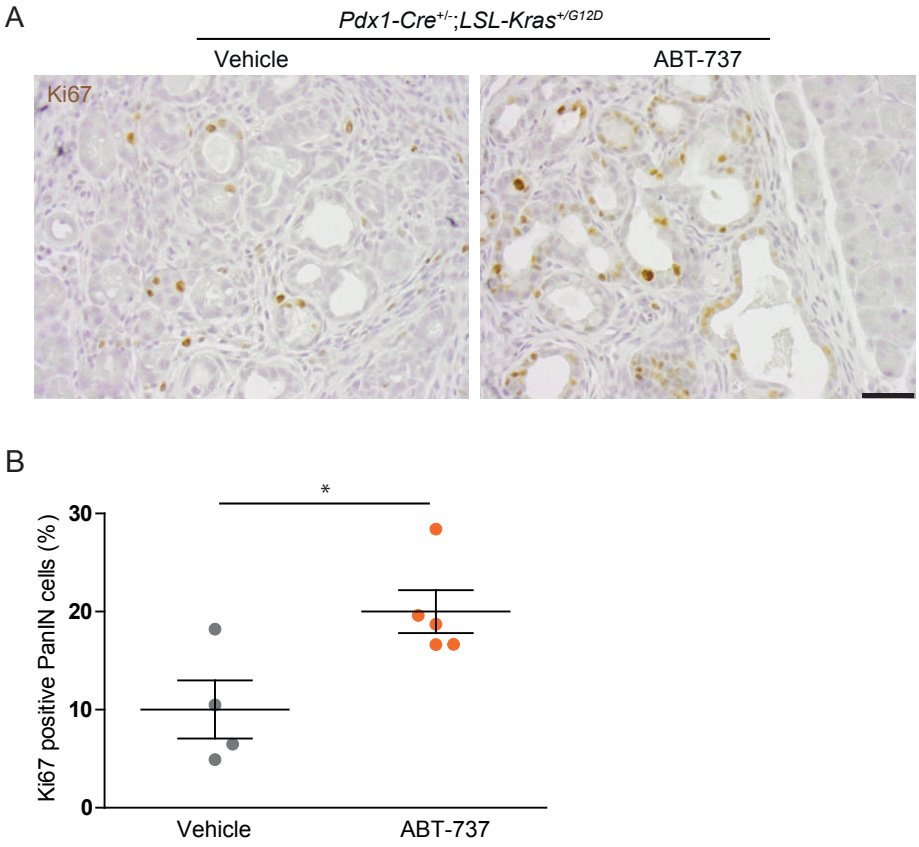

Figure S6. Bcl2-family protein inhibition by ABT-737 increases the percentage of Ki67⁺ cells in PanINs. *Pdx1-Cre*$^{+/-}$*;LSL-Kras*$^{+/G12D}$ mice were treated by caerulein at 2.5 months of age, followed by treatment with ABT-737 two weeks subsequently, and analyzed two days later. **A.** Representative images of pancreas sections from vehicle or ABT-737 treated mice stained for Ki67 (brown). **B.** Percentage of Ki67⁺ cells in PanINs from same mice. *, $P < 0.05$, **, $P < 0.005$, *t*-test.

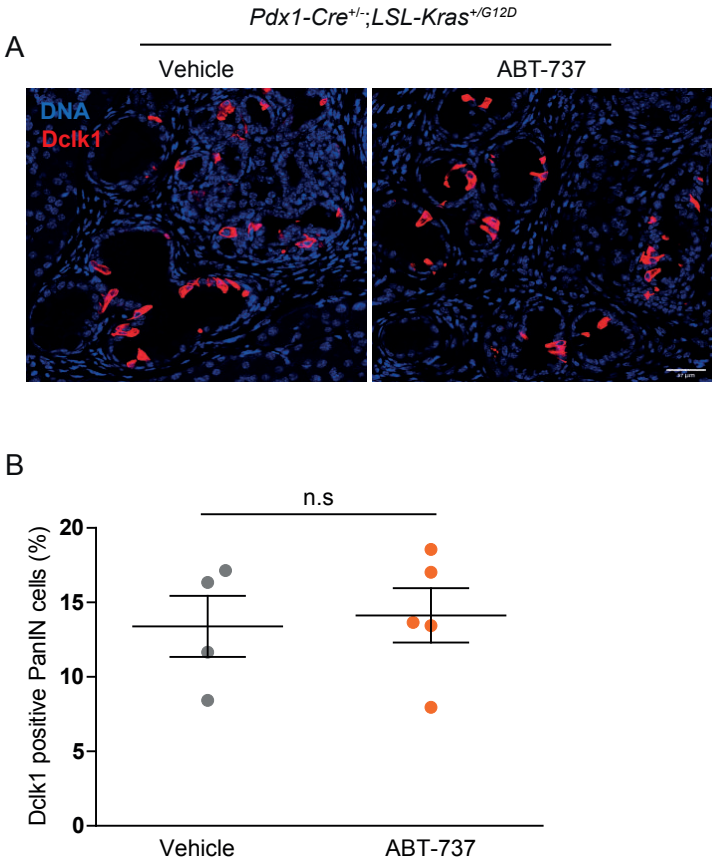

Figure S7. Bcl2-family protein inhibition by ABT-737 does not eliminate Dclk1$^+$ cells. *Pdx1-Cre$^{+/-}$;LSL-Kras$^{+/G12D}$* mice were treated by caerulein at 2.5 months of age, followed by treatment with ABT-737 two weeks subsequently, and analyzed two days later. **A.** Representative staining for Dclk1 in pancreas sections from vehicle and ABT-737 treated mice. **B.** Percentage of Dclk1$^+$ cells in PanINs from same mice. *, $P < 0.05$, **, $P < 0.005$, *t*-test.

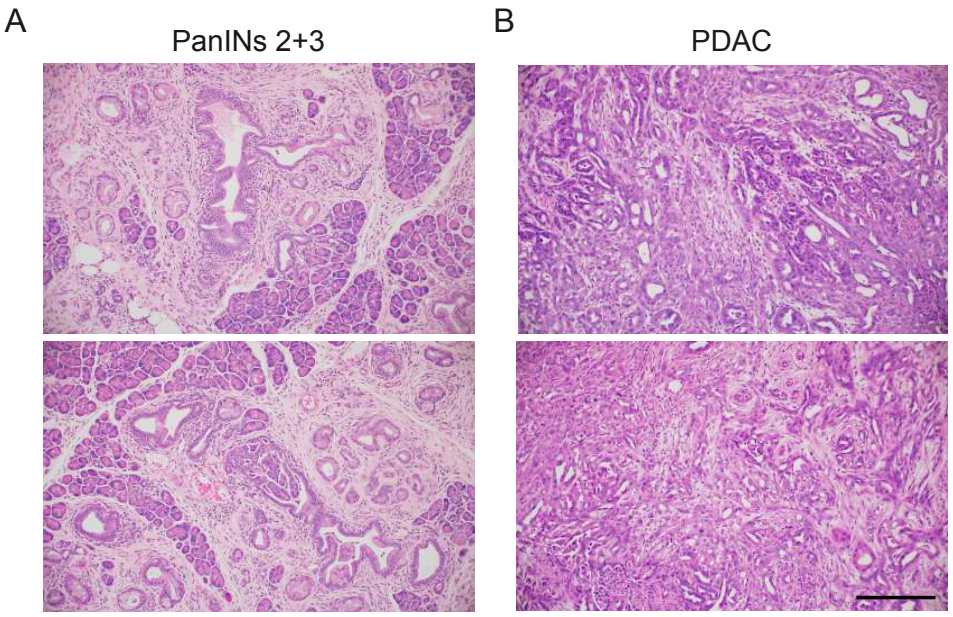

Figure S8. High grade PanINs and pancreatic carcinoma in *Pdx1-Cre$^{+/-}$;LSL-Kras$^{+/G12D}$* mice. Representative images of PanIN2 and PanIN3 lesions (panel A) and pancreatic ductal carcinoma (PDAC, panel B) observed in caerulein-treated *Pdx1-Cre$^{+/-}$;LSL-Kras$^{+/G12D}$* mice at 9 months of age. Lesions are from mice that did not receive ABT-737. Size marker = 200μm.